LANGMUIR

pubs.acs.org/Langmuir

Invited Feature Article

Uncovering the Underlying Mechanisms Governing the Solidlike Layering of Ionic Liquids (ILs) on Mica

Yali Wang* and Lei Li*

Cite This: *Langmuir* 2020, 36, 2743−2756

Read Online

ACCESS | Metrics & More | Article Recommendations

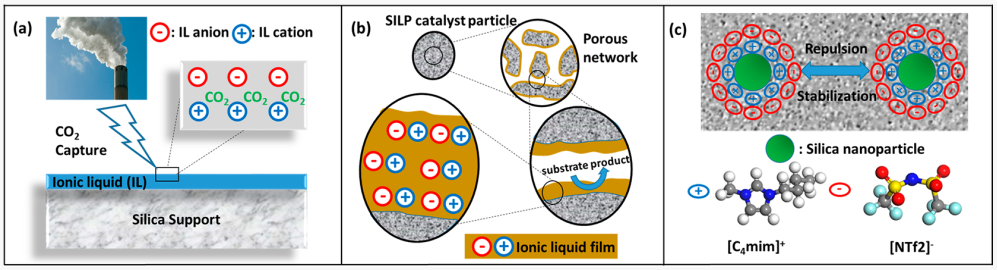

ABSTRACT: Significant progress has been made in understanding the IL−solid interface in the past three decades, and a key finding is that ILs can form solidlike layers at the interface. It has been recognized that the electrostatic forces at the solid−IL interface and self-assembly of ILs are key enablers of the IL layering. However, regarding the layering structure of ILs, research from different laboratories is not consistent; i.e., the number of solidlike layers could range from 0 to ∼60, indicating the complexity of the underlying mechanisms and/or the existence of overlooked key parameters. In the current review, we will discuss the underlying mechanisms and key parameters governing the layering of ILs on mica, the most studied model solid. First, we will present the experimental findings from various laboratories, both consistent and contradictory ones, and summarize the current understanding of the governing mechanisms. Then, we will discuss the possible key parameters, including the structure of ILs, surface modification and contamination of mica, and cosolvent impacting the solidlike layering of ILs. Finally, we will discuss future research directions in uncovering the underlying mechanisms.

INTRODUCTION

Ionic liquids (ILs), organic salts with the melting temperature below room temperature, have attracted increasing attention in the past three decades because of their exceptional physicochemical properties, e.g., nonvolatility, thermal and electrochemical stability, tunable polarity, and high ionic conductivity.[1−4] Due to the bulky and asymmetric geometry of the organic ions in ILs, electrostatic attraction and lattice-packing arrangements are depressed, leading to the low melting points for ILs.[5] In addition to electrostatic forces, other forces, such as hydrogen bonding and van der Waals and solvophobic forces also play a role in determining the properties of ILs.[4,6,7] Numerous applications of ILs involve solid−IL interfaces, and the structure of ILs at these interfaces are critical to their performance. For example, an IL is a good adsorbent for CO_2 capture (see Figure 1a).[4,8] Confining a nanometer-thick IL to porous solids, e.g., silica, overcomes the high cost, high viscosity, and low gas diffusion associated with bulk ILs and is a promising approach for large-scale operations.[4,8] At solid−IL interfaces, previous research[9] showed that the interfacial structure of IL ions, which is determined by both the chemical structure of the IL and IL−solid interaction, significantly impacts the CO_2 adsorption. Another example is present in supported ionic liquid-phase (SLIP) catalysts, which are produced by simply depositing thin IL films containing catalysts on a solid support such as silica, as shown in Figure 1b. Here, the negligible vapor pressure of ILs is crucial to achieving the immobilization of a nanometer-thick liquid layer on a solid support and makes it attractive for gas-phase reactions compared to conventional volatile organic solvents.[4,8,10] Previous research[11,12] indicated that the ion-level structure at solid−IL interfaces greatly impacts the stability and activity of the catalysts. In nanoparticle dispersions (Figure 1c), ILs have been exploited as promising dispersion media due to their unique solvation property,[13] and it has been found that silica nanoparticles are surprisingly stable in ILs, even without any surfactants. Although the exact mechanism is still under debate, it has been proposed that the layering of IL ions on the

Received: December 16, 2019
Revised: February 20, 2020
Published: February 26, 2020

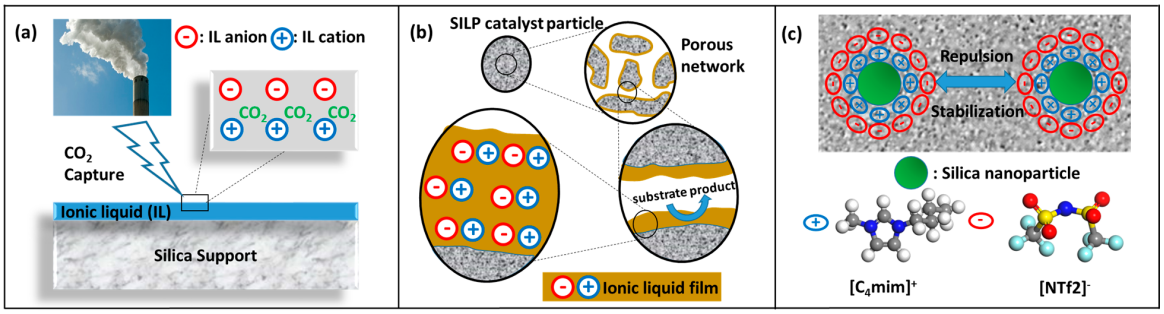

Figure 1. (a) Schematic of CO_2 capture with ILs. (b) Schematic of SLIP catalysis of a gas-phase reaction.[10] Reproduced with permission from ref 10. (Copyright 2005 American Chemical Society). (c) Schematic showing that the solidlike layering of IL induces long-range repulsion and thus stabilizes silica nanoparticles. The background is an optical image of a dispersion of silica nanoparticles in ILs.[14] Reproduced with permission from ref 14 (copyright 2009 American Chemical Society). Figures are not drawn to scale.

silica surface leads to a long-range repulsion that stabilizes the nanoparticles.[14]

Significant progress has been made in understanding the structure of ILs at the IL−solid interface in the past three decades, and a key finding is that ILs can form solidlike layers at the interface. To the best of our knowledge, though there have been several excellent reviews[4,5,8,15−17] on the IL−solid interface, no review article focusing on the solidlike layering of ILs on mica has been published to date. To address this, in this article, the solidlike layering of ILs on mica, the most frequently studied model solid surface due to its well-defined surface chemistry and availability,[18−22] will be reviewed with a focus on the experimental studies. First, the current research status of the solidlike layering of ILs on mica will be reviewed. Second, the important parameters affecting the solidlike layering will be discussed. Finally, future research directions to fully uncover the governing mechanisms will be outlined.

SOLIDLIKE LAYERING OF IL ON MICA: CURRENT STATUS

It is well known that the interfacial structure of molecular liquids confined to a solid surface is different from that in the bulk.[23−25] Mobile liquid molecules adjacent to the solid surface could form "solidlike layers" (often referred to as "solvation layers"), which usually extend to a few molecular diameters from the liquid−solid interface. This layering structure is characterized by an oscillatory density profile and has been observed for simple molecular liquids as well as polymer melts. It has been proposed that entropy is essential to the formation of solidlike layers since layering also occurs when there is no attractive solid−liquid interactions.[24,25] It has been proposed that, under spatial confinement when next to a solid wall, for liquid molecules the available translational entropy decreases so much that it becomes thermodynamically favorable for the molecules to form an ordered solidlike layered structure.[24] In this layering process, both the size and geometry of the liquid molecules are important because both parameters affect the packing efficiency. For ILs, the asymmetric and bulky ions are expected to decrease the packing efficiency. However, in 1988, Horn et al. conducted an SFA measurement of the oscillatory force of ethylammonium nitrate (EAN) confined between mica surfaces and reported that there are as many as nine solidlike layers of EAN on the mica surface.[26] Later, many others reported the existence of extended solidlike layering for ILs using a variety of characterization techniques, including X-ray reflectivity (XRR),[27,28] AFM topography,[19,29−32] AFM force−distance measurements,[5,18,33,34] the surface force apparatus (SFA),[20,35−40] and high-resolution X-ray interface scattering.[41]

Since those experimental works were conducted on mica and the mica surface carries negative charge,[42] it is generally accepted that electrostatic interactions are critical to the extended solidlike layering of ILs on mica,[29,35,37,43−46] though the exact mechanism, e.g., exact ionic structure of ILs, is still under debate.[16,44,47] Moreover, it has also been proposed that the self-assembly of ILs is another key contributing to the solidlike layering.[48] Because IL ions, e.g., cations, have a surfactant-like structure, the self-organization is expected to form separate polar and nonpolar domains. Indeed, both experimental[49−52] and computational[53,54] studies on bulk ILs indicated the existence of mesoscopic nanostructures, which demonstrates the self-assembling capability of ILs. At the IL−solid interface, the self-assembling of polar and nonpolar domains can promote the layered structure.

Although the interfacial electrostatic interaction and self-assembly mechanisms explain the extended solidlike layering of some ILs at the IL−mica interface, significant inconsistency exists among various reports (see Table 1), ranging from no layering to tens of solidlike layers even for the same IL. For example, using angle-resolved X-ray photoelectron spectroscopy (ARXPS), Deyko et al. found that there were no solidlike layers after $[C_4C_1Im][NTf_2]$ was deposited on the mica by physical vapor deposition.[55] In contrast, using an AFM topography study, Bovio et al. reported that there are 50-nm-thick solidlike layers of the same IL, which was deposited on mica by solution casting.[19] These contradictory results suggest the complexity of the governing mechanisms of the solidlike layering of IL at the IL−mica interface. They also imply that some key parameters could be missing.

PARAMETERS IMPACTING THE SOLIDLIKE LAYERING OF ILs

Previous research indicated that three parameters, i.e., the structure of ILs, surface modification, and the contamination of mica and the cosolvent, impact the solidlike layering significantly. In this section, these three parameters will be discussed in detail.

Structure of ILs. Previous research[5,18,35,38,39,56] showed that electrostatic interactions at the IL−mica interface and the self-assembly ability of ILs are the key factors impacting the solidlike layering of IL. On the negatively charged mica surface, the adsorption of the IL cation initiates the solidlike layering, and the self-assembly of the ILs promotes the growth of the solidlike

https://dx.doi.org/10.1021/acs.langmuir.9b03865
Langmuir 2020, 36, 2743−2756

Table 1. Solidlike Layering Structure of Ionic Liquids on Mica

cation	anion	characterization technique	thickness of solidlike layers (nm)	deposition methods and reference
C_4C_1Im	NTf_2	AFM topography	~50	solution casting of IL on mica with the solvent evaporated under a saturated atmosphere[19]
C_4C_1Im	NTf_2	SFA	6.6	neat IL confined between two mica surfaces[35,39]
C_4C_1Im	NTf_2	ARXPS	0	physical vapor deposition on mica under ultravacuum; dewetting occurs[55]
C_4C_1Im	NTf_2	frequency-modulation AFM	several (not specified)	neat IL on mica[21]
C_4C_1Im	NTf_2	X-ray interface scattering	3.5	neat IL on mica[45]
C_4C_1Im	FAP	AFM topography	17	dip-coating of IL on mica[31]
C_4C_1Im	FAP	AFM topography	0	mica was heated before dip-coating; dewetting occurs[31]
C_4C_1Im	PF_6	AFM topography	several (not specified)	solution casting of IL on mica with the solvent evaporated under an ambient atmosphere[32]
C_4C_1Im	PF_6	AFM topography	0	solution casting of IL on mica with the solvent evaporated under an ambient atmosphere; APTES-modified mica[32]
C_4C_1Im	PF_6	AFM force−distance	4.2	neat IL on mica[33]
C_4C_1Im	PF_6	SFA	4−5	neat IL between two mica surfaces[37]
C_4C_1Im	PF_6	SFA	0	neat IL between two OMCTS-modified mica surfaces[37]
C_4C_1Im	BF_4	SFA	5−6	neat IL between two mica surfaces[37]
C_4C_1Im	BF_4	SFA	0	neat IL between two OMCTS-modified mica surfaces[37]
C_4C_1Im	BF_4	frequency-modulation AFM	several (not specified)	neat IL on mica[21]
C_1C_1Im	NTf_2	ARXPS	0	physical vapor deposition on mica under ultravacuum; dewetting occurs[55]
C_2C_1Im	$EtSO_4$	SFA	1.1	neat IL confined between two mica surfaces[20]
C_2C_1Im	NTf_2	AFM force−distance	3.8−4.5	neat IL on mica[33]
C_2C_1Im	acetate	AFM force−distance	2	neat IL on mica[18]
C_6C_1Im	NTf_2	SFA	14.6	neat IL confined between two mica surfaces[35,39]
C_6C_1Im	$EtSO_4$	extended SFA	60	neat IL confined between two mica surfaces[34]
C_6C_1Im	$EtSO_4$	AFM force−distance	3	neat IL on mica[34]
$C_{10}C_1Im$	NTf_2	SFA	8	neat IL confined between two mica surfaces[40]
$C_{10}C_1Im$	NTf_2	neutron scattering	4	neat IL on mica[40]
C_4C_1Pyrr	NTf_2	SFA	4.5	neat IL between two mica surfaces[38,39]
C_6C_1Pyrr	NTf_2	SFA	4.8	neat IL between two mica surfaces[38,39]
C_8C_1Pyrr	NTf_2	SFA	4.9	neat IL between two mica surfaces[38,39]
$C_{10}C_1Pyrr$	NTf_2	SFA	8.5	neat IL between two mica surfaces[38,39]
$C_2H_5NH_3^+$	NO_3^-	AFM force−distance	3	neat IL on mica[5]
$C_2H_5NH_3^+$	$HCOO^-$	AFM force−distance	1	neat IL on mica[5]
$C_3H_7NH_3^+$	NO_3^-	AFM force−distance	3	neat IL on mica[5]
$C_3H_7NH_3^+$	$HCOO^-$	AFM force−distance	0.7−1	neat IL on mica[5]
$(CH_3)_2C_2H_5NH_3^+$	$HCOO^-$	AFM force−distance	0.5−0.8	Neat IL on mica.[5]
$(C_2H_5)(CH_3)NH_2^+$	$HCOO^-$	AFM force−distance	0.5−0.8	neat IL on mica[5]

layers. The geometry of the cation influences the registry of the cation on the mica charge sites and thus impacts the layering process. The self-assembly ability is determined by the structure of both cations and anions, which changes the electrostatic force, hydrogen bonding between polar groups, and dispersion force between the cation alkyl chains.

Using SFA, Perkin et al. systematically investigated the interfacial structure of imidazolium- and pyrrolidinium-based aprotic ILs, i.e., $[C_nC_1Im][NTf_2]$ with n = 4, 6 and $[C_nC_1Pyrr][NTf_2]$ with n = 2, 4, 6, 8, 10, confined between two negatively charged mica surfaces.[35,38,39] In all cases, they observed the solidlike layering and concluded that such layering results from the negative charge of the mica surface, which attracts the cation of the ILs and thus initiates the layering process. For imidazolium-based ILs, they found that the length of the alkyl chain in the cation is the key to the structure of the solidlike layers. As shown in Figure 2, the oscillatory force profile indicates that shorter alkyl chains result in an alternating cation−anion monolayer, while longer alkyl chains result in a cation bilayer structure. The bilayer structure is similar to conventional surfactants, in which polar and nonpolar domains coexist. Interestingly, there are two major differences between imidazolium- and pyrrolidinium-based ILs. First, the crossover from monolayer to bilayer occurs at different chain lengths: the crossover point for $[C_nC_1Im][NTf_2]$ is 4−6, while it is 8−10 for $[C_nC_1Pyrr][NTf_2]$. (See Figures 2 and 3.) This difference has

https://dx.doi.org/10.1021/acs.langmuir.9b03865
Langmuir 2020, 36, 2743−2756

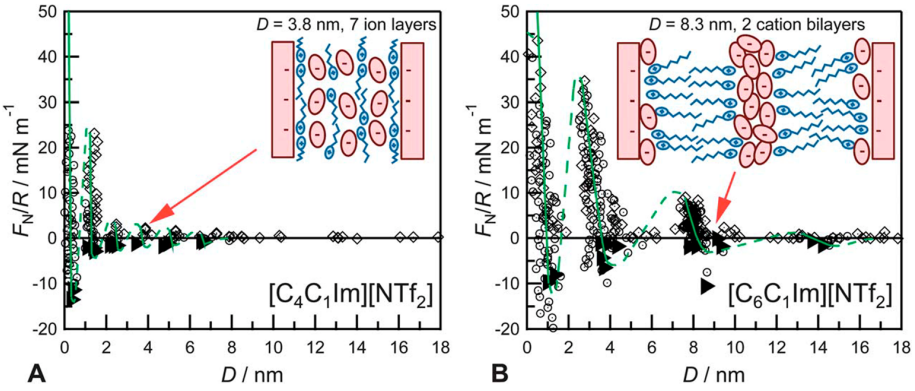

Figure 2. Measured normal force, FN, normalized by the radius of curvature, R, between mica surfaces across (A) $[C_4C_1Im][NTf_2]$ and (B) $[C_6C_1Im][NTf_2]$ as a function of surface separation, D. Schematics indicate the likely ion layering structures, showing example film configurations for the repulsive walls indicated consisting of alternating cation/anion monolayers for $[C_4C_1Im][NTf_2]$ and toe-to-toe cation bilayers for $[C_6C_1Im][NTf_2]$. Reproduced with permission from ref 39 (copyright 2013 Royal Society of Chemistry).

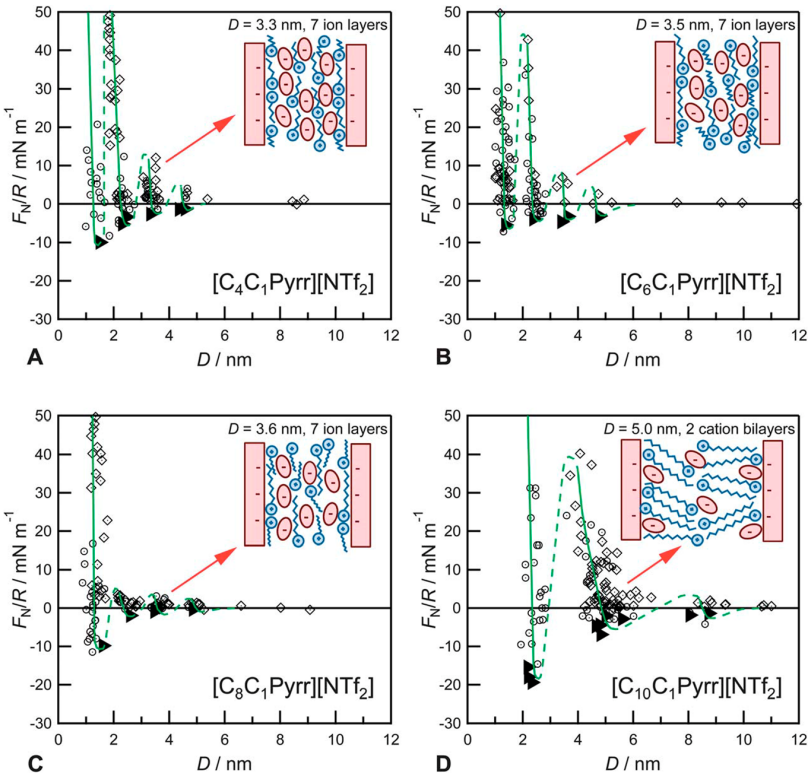

Figure 3. Measured normal force, FN, normalized by the radius of curvature, R, between mica surfaces across (A) $[C_4C_1Pyrr][NTf_2]$, (B) $[C_6C_1Pyrr][NTf_2]$, (C) $[C_8C_1Pyrr][NTf_2]$, and (D) $[C_{10}C_1Pyrr][NTf_2]$ as a function of surface separation, D. Schematics indicate the likely ion layering structures, showing example film configurations consisting of alternating cation/anion monolayers for $[C_nC_1Pyrr][NTf2]$, where n = 4, 6, 8, and interdigitated cation bilayers for $[C_{10}C_1Pyrr][NTf_2]$. Reproduced with permission from ref 39 (copyright 2013 Royal Society of Chemistry).

been attributed to the different packing capability of two cations. Imidazolium rings can pack closely via $\pi-\pi$ stacking and thus render the aggregation of alkyl chains easier. In contrast, pyrrolidinium rings are aliphatic in nature and cannot pack closely via $\pi-\pi$ stacking. As a result, longer alkyl chains are required to form the nonpolar domain in the bilayer. Second, the bilayer for imidazolium-based ILs has toe-to-toe structure, i.e., anion/cation/cation/anion. However, for pyrrolidinium-based ILs, the alkyl chains are significantly tilted, and the $[NTf_2]$ anions are located between the cation headgroups, i.e., anion/cation/anion/cation. The difference here has also been attributed to the different packing efficiency of cation rings. Since imidazolium rings pack closely, they exclude the anions from the nonpolar region, thus resulting in toe-to-toe structure. For pyrrolidinium rings, they do not pack closely, which encourages the anions to intercalate between the cation rings.

Atkin et al.[5,18,56] examined the interfacial structure of ammonium protic ILs on mica utilizing the AFM force–

https://dx.doi.org/10.1021/acs.langmuir.9b03865
Langmuir 2020, 36, 2743−2756

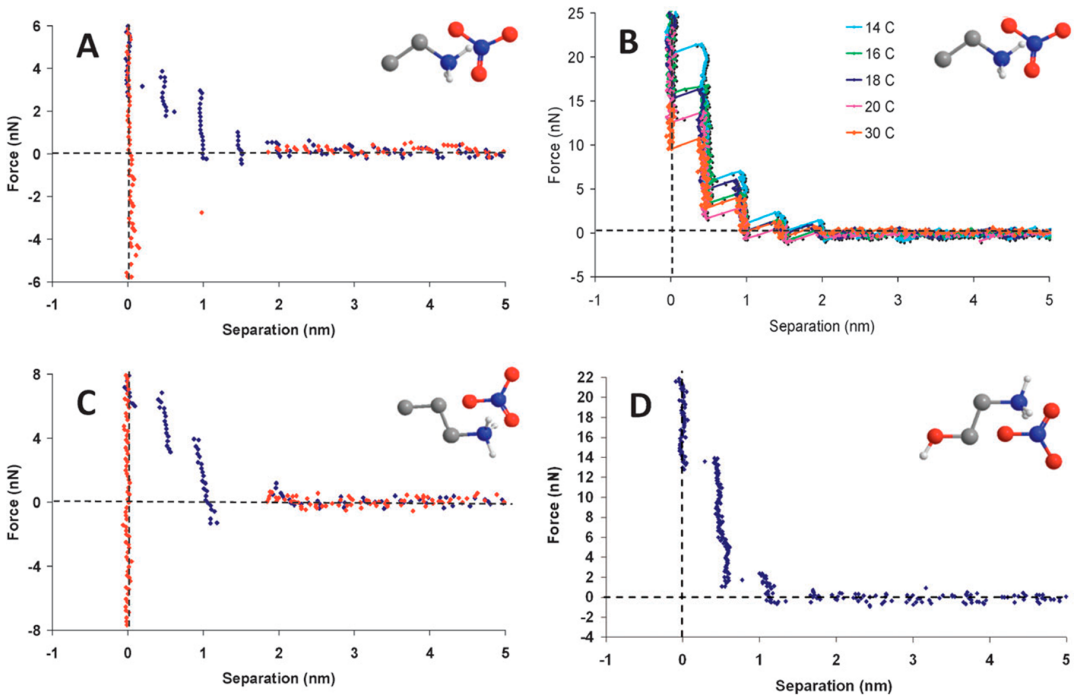

Figure 4. Force versus distance profile for an AFM tip approaching (blue) and retracting from (red) a mica surface in various protic ILs (A) EAN at 21 °C. (B) EAN at various temperatures. The forces here are directly comparable as the same Si_3N_4 tip was used in all temperature experiments. (C) PAN at 21 °C. (D) EtAN at 21 °C. Reproduced with permission from ref 5 (copyright 2010 Royal Society of Chemistry).

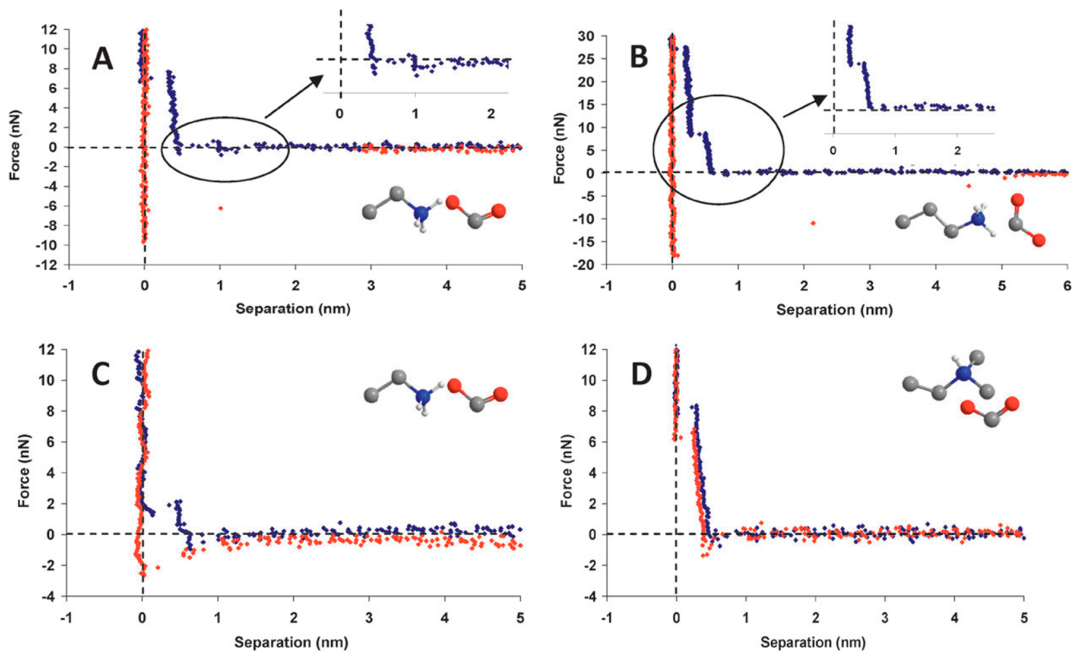

Figure 5. Force versus distance profile for an AFM tip approaching (blue) and retracting from (red) a mica surface at 21 °C in (A) EAF, (B) PAF, (C) EMAF, and (D) DMEAF. Reproduced with permission from ref 5 (copyright 2010 Royal Society of Chemistry).

distance profile. As shown in Figure 4A, for ethylammonium nitrate (EAN) they found six to seven alternating cation/anion layers and the innermost layer is the ammonium cation, neutralizing the negative charge of the mica surface. Interestingly, as shown in Figure 4B, increasing temperature decreases the number of solidlike layers, which has been attributed to the increased thermal motion disrupting the layering of ILs. Atkin et al. also found that replacing the ethyl group in EAN with a longer propyl group, i.e., propylammonium nitrate (PAN), results in fewer (4 in PAN vs 6−7 in EAN) and

https://dx.doi.org/10.1021/acs.langmuir.9b03865
Langmuir 2020, 36, 2743−2756

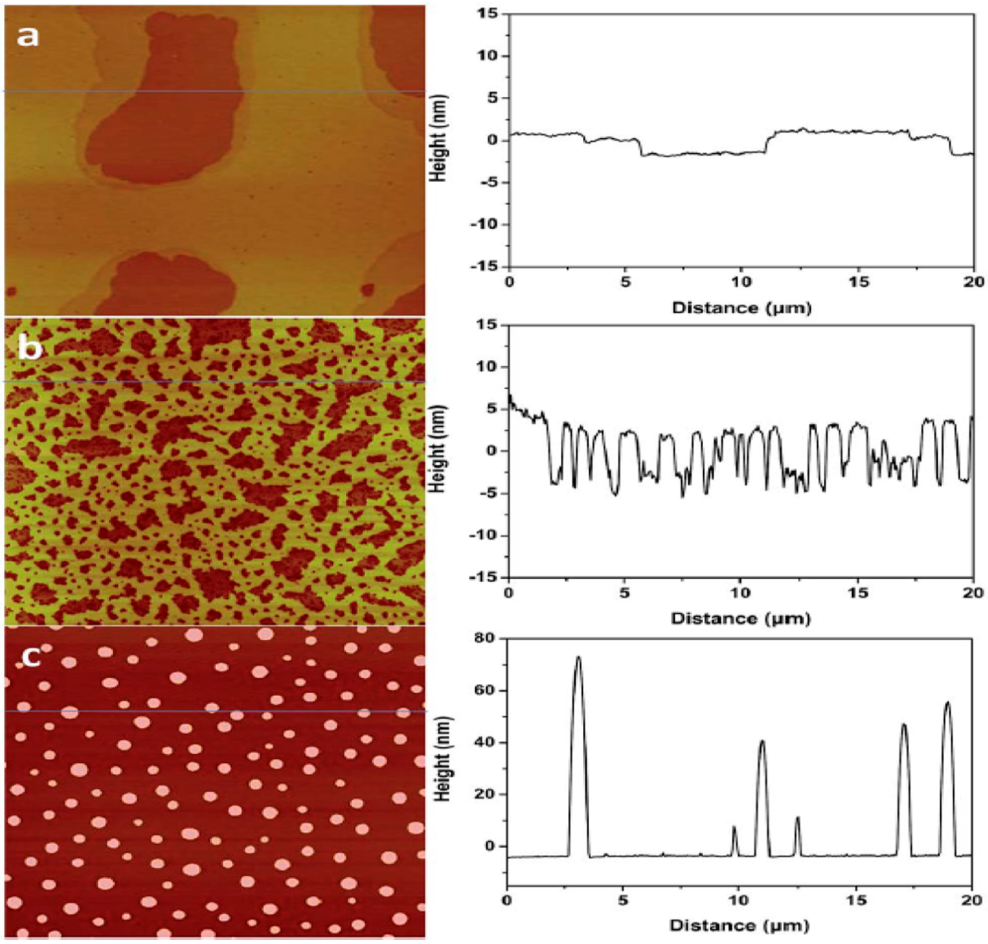

Figure 6. (Left) AFM images of $[C_4C_1Im][FAP]$ (1 g L^{-1} solution) dip-coated on a freshly cleaved mica surface (a), mica heated for 5 min at 120 °C (b), and mica heated for 1 h at 120 °C (c). AFM images are 20 μm × 20 μm, and the height bar is 20 nm. (Right) Corresponding line profiles. Reproduced from ref 60 (copyright 2015 Royal Society of Chemistry).

more compressible layers. (Figure 4C) They proposed that this is because the propyl group has more rotational freedom and thus packs more efficiently without layering. As shown in Figure 4D, when a hydroxyl group is introduced to the alkyl chain of the cation (EtAN), fewer solidlike layers are detected. This has been explained by the lower melting point of EtAN, similar to the discussion above on the temperature effect. When the nitrate anion is replaced with a formate anion, as shown in Figure 5A,B, fewer and more compressible solidlike layers are observed. Atkin et al. has attributed the change to lower melting points of the IL containing formate anion. As shown in Figure 5C,D, only a single solidlike layer is observed for the ILs with secondary and tertiary ammonium cations, which has been attributed to the steric hindrance preventing the cations from closely approaching the mica substrate. As a result, the strength of electrostatic interactions between the cations and the mica binding sites is reduced. Meanwhile, hydrogen bonding network formation is limited due to fewer available hydrogen atoms in the secondary and tertiary ammonium cations.[5,18,56]

More recently, utilizing amplitude modulation (AM) AFM, Atkin et al.[57] studied the lateral structure of several protic ILs on mica. They found that the structure of the innermost layer is primarily determined by the registry between cation and mica charge sites. For primary ammonium ILs, the innermost ion layer, i.e., cation, is electrostatically bound to the mica and relatively immobile. For bulky DMEA cations, since it is difficult for them to approach the surface charge site, the lateral structure of the innermost layer is much weaker. In bulk protic ILs, electrostatic force and hydrogen bonding between charged groups and the dispersion force between cation alkyl chains results in a solvophobic segregation into polar and nonpolar domains. Interestingly, Atkin et al. found that the near-surface IL structure in a lateral direction is similar to that of bulk IL. However, it shows a compromise between the bulk IL liquid and the surface layer. In other words, the near-surface layer exhibits a flattening and lateral extension of the bulk structure. As expected, the lateral layering structure is affected by both the anion and cation structures.[57] In another study by the same group, it was also found that[58] there is a correlation between the bulk structure and the lateral surface structure of the ILs. Different from protic EAN, aprotic $[C_2C_1Im][NTf_2]$ has weak self-assembly structure in the bulk. Interestingly, it shows only discrete ions on the mica surface where EAN exhibits an ordered wormlike pattern. The different lateral structures of EAN and $[C_2C_1Im][NTf_2]$ have been attributed to their different abilities to self-assemble. The stronger electrostatic interactions between localized charged group, i.e., ethylammonium, and the surface charge sites as well as the hydrogen bonding network in EAN

https://dx.doi.org/10.1021/acs.langmuir.9b03865
Langmuir 2020, 36, 2743−2756

promote its self-assembly. For $[C_2C_1Im][NTf_2]$, the electrostatic interactions between the surface charge sites and delocalized $[C_2C_1Im]^+$ are much weaker.[58]

Surface Modification/Contamination of Mica. Since the electrostatic interaction at the IL−mica interface is critical to the solidlike layering of ILs, the surface chemistry of the mica plays an important role. The mica crystal has one octahedral layer of aluminum and two tetrahedral layers of silicon sandwiched between potassium layers. An atomically smooth mica surface can be easily prepared by cleaving a sheet of mica along the (001) plane with half of the potassium on each cleaved face.[31] It is expected that the ion exchange between the cation of the IL and K^+ on mica is the critical step in initiating the solidlike layering of ILs. One way to confirm the idea is to block the cation−K^+ exchange and see how it impacts the solidlike layering. Indeed, Liu et al.[32] showed that the solidlike layers of $[C_4C_1Im][PF_6]$ on mica completely disappear and dewetting, i.e., a droplet, occurs when 3-aminopropyl-triethoxysilane (APTES) is attached to the mica. They[32] attributed the dramatic change to the fact that, on APTES-modified mica, the cation−K^+ exchange is not possible. Bou-Malham et al.[37] reported very similar results: the solidlike layers of $[C_4C_1Im]$-$[BF_4]$ on mica disappear when the IL is in contact with the octamethylcyclotetrasiloxane (OMCTS)-modified mica surface.

The freshly cleaved mica surface is hydrophilic[59] and readily absorbs water, e.g., up to a few angstroms,[60] under ambient conditions. Interestingly, recent research suggested that the adsorbed water on the mica could be critical to the cation−K^+ exchange and the solidlike layering of mica. On the basis of the AFM and ATR-FTIR results, Gong et al.[60] showed that $[C_4C_1Im][FAP]$ forms solidlike layers when water is adsorbed on the mica surface under ambient conditions. However, when the water is removed by heating at elevated temperatures, instead of solidlike layers, ILs exhibit droplet structure on mica. As shown in Figure 6a, when the mica is cleaved under ambient conditions (22 °C, RH = 45%) right before $[C_4C_1Im][FAP]$ is deposited on mica by dip-coating, the solidlike layers are clearly visible. However, when the freshly cleaved mica was held at 120 °C for 1 h to remove the water, the solidlike layers completely disappeared and droplets were observed (Figure 6c)! ATR-FTIR results[60] confirmed that there is adsorbed water on mica before heating and significant amounts of water are removed after heating.

To explain why the adsorbed water on mica promotes solidlike layering, Gong et al.[60−62] proposed two possible mechanisms as schematically shown in Figure 7. The first one is water-enabled surface charging. Because the dielectric constant of ILs is low,[63] ILs are not expected to dissolve K^+ ions on mica effectively. Therefore, the surface charging of mica cannot occur. Only after water, i.e., an effective solvent, adsorbs on the mica, K^+ ions will be effectively dissolved and leave the surface of mica. As a result, the surface will carry negative charges and the cations of the IL will occupy the "empty" site left by K^+, which initiates the solidlike layering. The second proposed mechanism is water-assisted self-assembly. For bulk ILs, previous research[64,65] showed that the water and IL ions are coupled via H-bonding, which leads to a more extended polar network, i.e., a stronger self-assembly of ILs. At the IL−mica interface, since the mica serves as a flat template initiating the packing of ILs, the water-assisted self-assembly of IL promotes the extended solidlike layering.

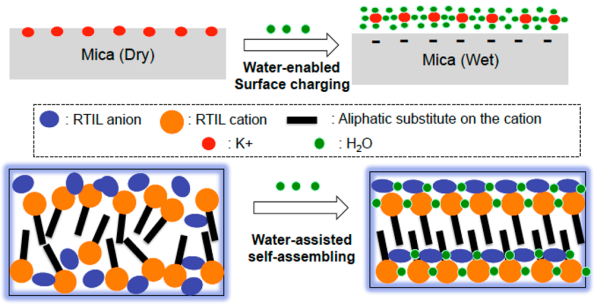

Figure 7. Schematic of the effect of adsorbed water on the solidlike layering of room-temperature IL (RTIL) on the mica surface.[61] Reproduced with permission from ref 61 (copyright 2017 Elsevier).

Previously, Deyko et al.[55] showed that, under ultrahigh vacuum, dewetting occurs to $[C_4C_1Im][NTf_2]$ on a clean mica surface and no solidlike layering of the IL was observed. However, Bovio et al. found that[19] exactly the same IL exhibits extensive solidlike layering on mica under ambient conditions. The puzzling results now can be explained if the adsorbed water on mica is the missing key parameter in solidlike layering: there is no water under ultrahigh vacuum. This idea was also echoed by Cheng et al.[59,66] in their AFM force−distance and SFA studies. They found that adding water to ILs, instead of onto the surface of mica, promotes the solidlike layering of ILs on mica and concluded that the enhanced layering results from the water-enabled surface charging. The results[59,66] suggest that adsorbed water from bulk IL could also contribute to the layering of IL on mica. Wang et al.[67] and Gong et al.[62] reported that high humidity promotes the macroscopic wetting of $[C_2C_1Im][NTf_2]$ and $[C_4C_1Im][NTf_2]$ on mica and attributed the increased wettability to the water-enabled surface charging and the resulting layering process. (See Figure 8.) More recently, Lhermerout et al.[68] conducted the surface force balance study and found that humidity improves the mechanical resistance of the solidlike layers of $[C_4C_1Pyrr][NTf_2]$. They attributed the higher resistance to the better dissolution of the K^+ ions on the mica, which results in more ordered layering. This result also supports the idea proposed by Gong et al.[60−62]

Although the above-mentioned results[59−62,66−68] support the idea that water is the key to the surface charging of mica and the solidlike layering of ILs, there have been different voices. On the basis of the amplitude-modulated atomic force microscopy (AM-AFM) study of the metal ion adsorption in propylammonium nitrate (PAN) on mica, McDonald et al.[57,69] reported that the solvation of K^+ occurs when dry PAN is in contact with mica, challenging the idea proposed by Gong et al.[60−62] that the desorption of K^+ cannot occur without water. The reason for the controversy remains unclear. However, there are two points worth further study. First, Gong et al.[60−62] studied a very hydrophobic IL, i.e., $[C_4C_1Im][FAP]$, while McDonald et al.[57,69] studied a hydrophilic IL, i.e., PAN. Second, the amount of adsorbed water on the mica surface (under ambient conditions) might be very different, e.g., different relative humidity (RH), between the two studies.

Cosolvent. The mixture of IL with molecular solvents is important in many applications. For example, the conductivity of IL solution can be effectively tuned by adding cosolvents.[70] It has also been found that the presence of water in cyano-based ILs impairs their tribological performance.[71] The fundamental interaction between IL and molecular solvent and the solvation dynamics have attracted a lot of research interest.[72−74]

https://dx.doi.org/10.1021/acs.langmuir.9b03865
Langmuir 2020, 36, 2743−2756

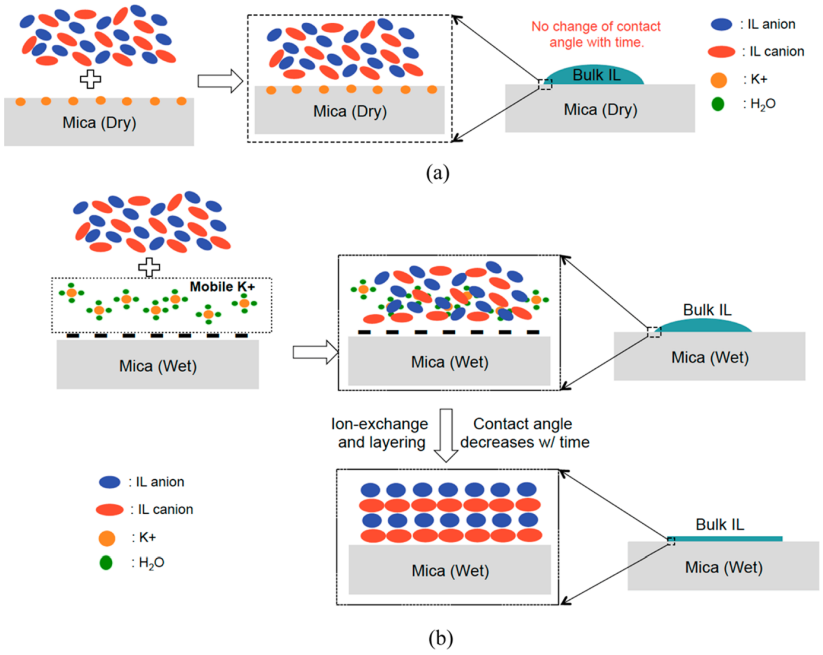

Figure 8. Proposed mechanisms illustrating the effect of adsorbed water on the molecular arrangement and wetting of ILs on the mica surface. (a) Dry mica (top). (b) Wet mica (bottom). Reproduced with permission from ref 62 (copyright 2018 America Chemical Society).

Regarding the layering of ILs, several groups[26,59,66,75−79] have reported that the solidlike layering of ILs on mica changes with the addition of cosolvents, e.g., water, propylene carbonate, and polyoxyethylene alkyl ether. This research suggests that the key parameters impacting the solidlike layering include the molecular size, the chemistry, and the concentration of the cosolvent. The cosolvent could change the solidlike layering of ILs by changing the packing efficiency of the IL molecules and/or the surface charging of the mica. The competition of these two factors could explain some of the controversy in the existing literature.

On the basis of an SFA study, Horn et al.[26] reported that the number of solidlike layers of hydrophilic ethylammonium nitrate (EAN) decreases dramatically with the addition of water (50%), e.g., from eight to two layers, as shown in Figure 9. The authors attributed the decrease to the difference in the molecular size of water and EAN. A similar phenomenon has been observed for a mixture of nonpolar molecular liquids. When two liquids have different sizes, there will be more possible ways to fill the space so that the ordered layering structure is disrupted. More recently, Sakai et al.[75] studied the effect of water on the solidlike layering of a hydrophilic IL, i.e., $[C_4C_1Im][BF_4]$, and a hydrophobic IL, i.e., $[C_4C_1Im][NTF_2]$, on mica with an AFM force−distance profile. They found that, in both cases, the addition of water disrupts the solidlike layering of ILs. Interestingly, as shown in Figure 10, they concluded that there is an interfacial water phase formed on mica for the hydrophobic IL but not the hydrophilic one. They attributed this to the repulsion between the hydrophobic IL and water. Later, Wang et al.[76] and Jurado et al.[77] reported similar findings on $[C_xC_1Im][NTf2]$ and $[C_6C_1Im][EtSO_4]$, respectively, on mica. Sakai et al.[78] also investigated a ternary mixture of IL $[C_4C_1Im][BF_4]$, polyoxyethylene alkyl ether surfactant ($C_{12}E_6$), and water on mica via an AFM force−distance profile. They found that both the number and magnitude of oscillating layers decrease with increasing water concentration at a fixed surfactant ($C_{12}E_6$) concentration.

All the above-mentioned studies[26,75−78] showed that the addition of water disrupts the solidlike layering on the mica surface. However, based on the AFM force−distance profile shown in Figure 11, Cheng et al.[59] concluded that the addition of water to a hydrophobic IL, i.e., $[C_2C_1Im][NTf_2]$, promotes the solidlike layering of the IL on mica. Later, the same authors[66] also found similar results on another hydrophobic IL, i.e., $[C_8C_1Im][NTf_2]$. They attributed the enhanced solidlike layering to the water-enabled surface charging.[59,66] The reasons for the inconsistency between Cheng et al.[59,66] and others[26,75−77] remain unclear at this point. Gong et al.[60−62] proposed that water enhances the solidlike layering via water-enabled surface charging and water-assisted self-assembly. Horn et al.[26] proposed that water disrupts the solidlike layering due to the difference in size between water and IL. These two competing mechanisms could explain the controversy since the net effect of water could be highly dependent on the structure of the IL and the concentration of the IL−water mixture.

In addition to water, the effect of other solvents has also been studied since pure ILs are often mixed with polar solvents to lower their viscosity in order to increase the conductivity.[80] Smith et al.[79] studied a mixture of $[C_4C_1Im][NTF_2]$ and propylene carbonate confined between two mica surfaces with SFA. As shown in Figure 12, they found that the solidlike layering exists regardless of the composition of the mixture. However, the step size in the force curve, i.e., the thickness of the layer, goes through a transition with a threshold concentration of 30−35 mol % IL. Below the threshold, the step size, i.e., ∼0.55 nm, is the size of propylene carbonate. Above the threshold, the step size, i.e., ∼0.8 nm, is the size of the cation/anion IL pair. The finding here is clearly very different from that in the mixture of water and ILs, where the water itself does not show observable

https://dx.doi.org/10.1021/acs.langmuir.9b03865
Langmuir 2020, 36, 2743−2756

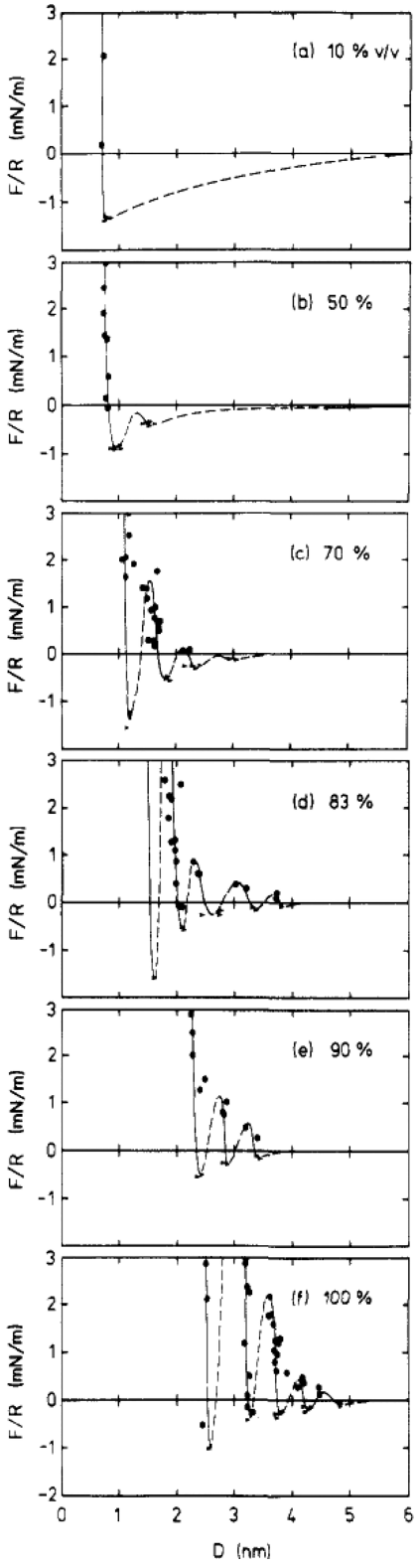

Figure 9. Forces measured in concentrated ethylammonium nitrate (EAN) solutions. The volume fractions are (a) 10, (b) 50, (c) 70, (d) 83, (e) 90, and (f) 100%, i.e., pure molten salt. Because a spring is used to measure the forces, there is an instability that causes the surfaces to jump outward from minima in the force curve.[17] These points are shown as arrowheads. Those parts of the force curve that have a positive slope are inaccessible and so are shown as dashed lines. Filled circles are measured points that must lie on stable regions of the curve, indicated by solid lines. Reproduced with permission from ref 26 (copyright 1988 American Chemical Society).

solidlike layering. This difference could be attributed to the fact that water shows high fluidity when confined to the mica surfaces[81,82] and thus does not form solidlike layers.

CONCLUSIONS

Although the underlying mechanism governing the solidlike layering structure of ILs at the IL−mica interface has not been fully uncovered, the progress and its implications in various applications are exciting. The electrostatic interaction at the IL−solid interface and the self-assembly of ILs, i.e., segregation of polar and nonpolar domains, are two key mechanisms. Many parameters, including the chemical structure of the cation and anion of ILs, the surface modification/contamination, and the cosolvents, impact the solidlike layering via these two mechanisms.

FUTURE OUTLOOK

Moving forward, there are still critical questions to be addressed to completely understand the underlying mechanisms.

First, how will the kinetic factor, i.e., the mobility of ILs, impact the solidlike layering of ILs? It is unclear at this point whether the observed solidlike layering in different studies is an equilibrium state. Given the fact that the bulk viscosity of ILs is much higher than that of molecular liquids, it is expected that the mobility of the IL is low, which is especially true when the IL is confined to a solid surface such as mica. Therefore, it is possible that the interfacial structure of ILs, after deposition or under mechanical stress, will change with time.[83,84] However, no systematic study has been conducted to address the possible kinetic effect. A good starting point will be the thermal annealing study. It will be interesting to see whether the solidlike layering will change with the annealing temperature and time. Since the thermal stability of ILs is high, the decomposition or evaporation of ILs is not a concern here. Another valuable study will be on the effect of the deposition method. When the IL is applied to the mica via solution casting or dip-coating, the existence of solvents is expected to increase the mobility of the IL and thus change the interfacial structure of the IL. A careful study of the chemistry and the evaporation rate of the solvent will provide insight into the possible kinetic effect.

Second, it is highly desirable to experimentally characterize the surface charging of mica in contact with dry and wet ILs. It has been generally accepted that the electrostatic force at the IL/mica interface is critical to the solidlike layering. However, the exact surface charging mechanism is still under debate. At this point, there is no consensus on whether the dissociation of K^+ is dependent on the adsorption of water at the interface. Since water adsorption is inevitable in many applications, it is essential to address this issue. Zeta potential measurements of the mica in contact with dry and wet ILs will be a good start to uncovering the mechanism. It is important to point out that the surface condition of mica needs to be carefully controlled and documented since mica readily adsorbs water under ambient conditions. As a result, a dry IL does not necessarily guarantee a dry IL−mica interface. Moreover, it will be interesting to extend

https://dx.doi.org/10.1021/acs.langmuir.9b03865
Langmuir 2020, 36, 2743−2756

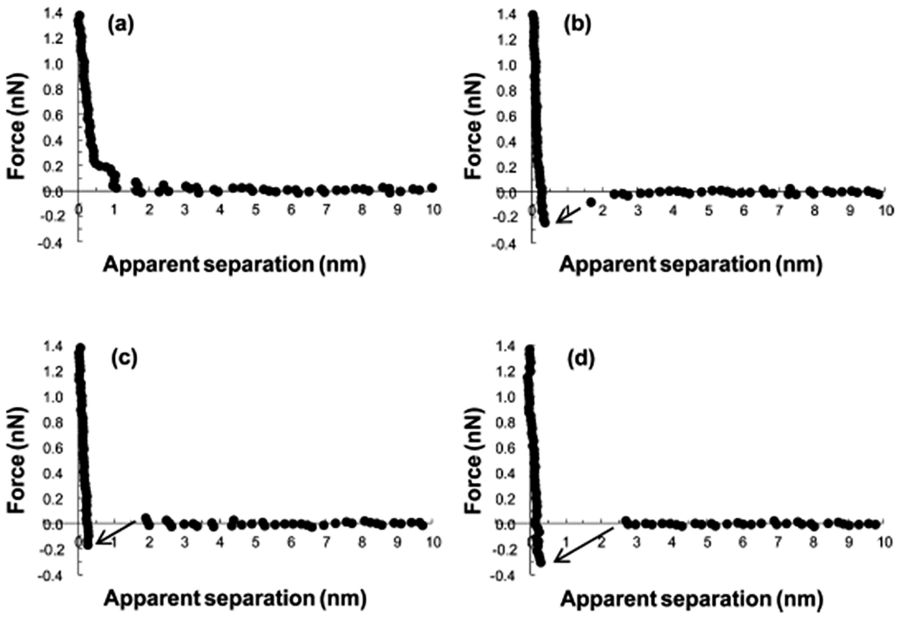

Figure 10. Inward force curves measured in $[C_4C_1Im][NTF_2]$ with and without added water. The solid substance employed here is mica, and the water concentrations measured by the Karl Fischer method are (a) 3 X10^{-4}, (b) 1.2, (c) 1.4, and (d) 2.0 wt % (saturation level). Reproduced with permission from ref 75(copyright 2015 America Chemical Society).

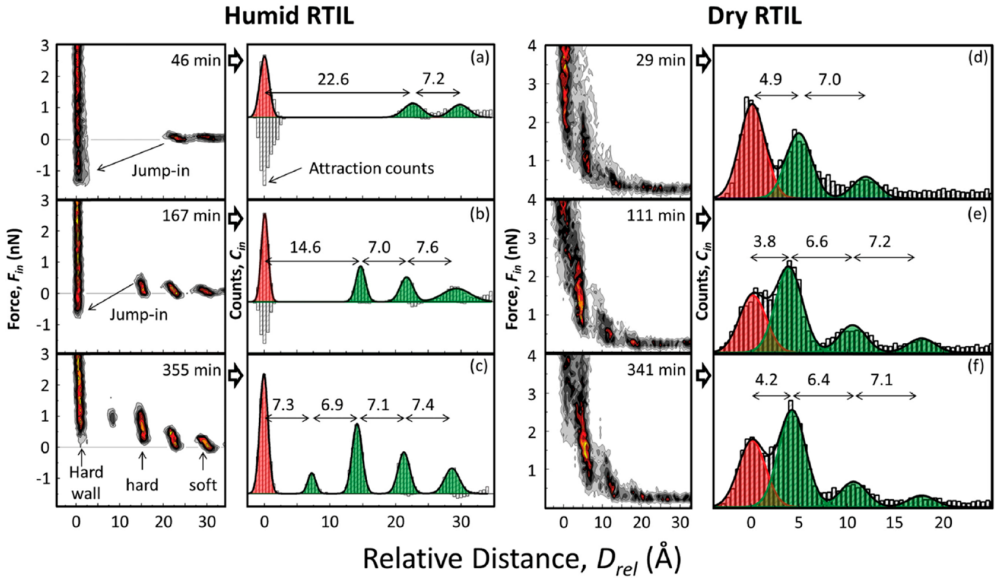

Figure 11. Interfacial IL layering characteristic of (a−c) humid and (d−f) dry $[C_2C_1Im][NTf_2]$ ionic liquid over 6 h. Layering histograms are generated from the 2D force versus relative distance probability density plots that are shown to the left of each layering histograms. All of the 2D population plots were generated from 40 randomly selected forces versus distance measurements. Reproduced with permission from ref 59 (copyright 2015 John Wiley and Sons).

the research from IL/water to other IL/solvent mixtures for two reasons. First, IL/solvent mixtures are important in many applications. Second, elucidating the solvent effect will help us to uncover the governing mechanisms of the surface charging of mica.

Finally, it is essential to obtain more detailed information on the arrangement of ions of IL in the solidlike layers. To date, the exact molecular structure of ILs in the solidlike layers remains unclear. Much controversy exists regarding the molecular orientation of the IL ions in the solidlike layers. One of the important reasons for the inconsistency is due to the limitation of individual characterization techniques. Physical characterization techniques, e.g., AFM, SFA, and XRR, directly show the existence of the IL layers and measure the thickness of the layers. However, they do not provide *direct* information on the arrangement of the IL ions within the layer. Meanwhile, chemical characterizations, such as XPS and SFG, directly probe the molecular arrangement of IL ions, but they cannot provide

https://dx.doi.org/10.1021/acs.langmuir.9b03865
Langmuir 2020, 36, 2743−2756

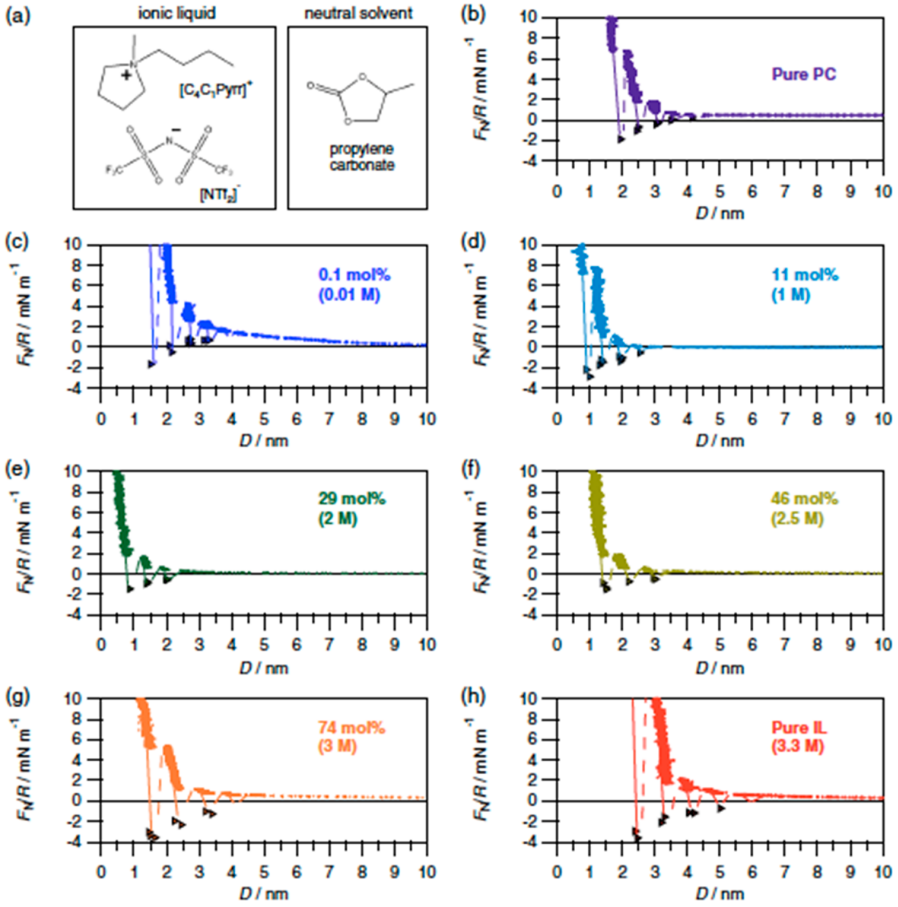

Figure 12. (a) Chemical structures and (b–h) measured forces F_N between two mica surfaces (normalized by radius of curvature R) as a function of surface separation D across liquids with concentrations ranging from pure propylene carbonate to a pure ionic liquid. Concentration values correspond to actual concentrations injected into the SFB rather than derived from a fit to data. Colored dots indicate repulsive forces measured on approach of the surfaces, and triangles indicate points measured from the jump apart from the surfaces from adhesive minima. Lines are a guide to the eye to show the oscillatory nature of the forces, with solid lines through the measured regions and a dashed line through regions inaccessible to measurement. Reproduced with permission from ref 79 (copyright 2015 American Physical Society).

direct information about the existence and the thickness of IL layers. Therefore, it is highly desirable to investigate the IL–mica interface using both physical and chemical techniques. Related to this, it will be interesting to further investigate the effect of water on the self-assembly of ILs, e.g., with different alkyl chains on the cation. Neutron reflectivity (NR) and ATR-FTIR are promising techniques to characterize the distribution of water in the IL layers and thus uncover how water affects the self-assembly of ILs.

AUTHOR INFORMATION

Corresponding Authors

Yali Wang – *Department of Chemistry and Chemical Engineering, Yulin University, Yulin, Shaanxi, P.R. China 719000; Department of Chemical & Petroleum Engineering, Swanson School of Engineering, University of Pittsburgh, Pittsburgh, Pennsylvania 15261, United States*; Email: yaw32@yulinu.edu.cn

Lei Li – *Department of Chemical & Petroleum Engineering, Swanson School of Engineering, University of Pittsburgh, Pittsburgh, Pennsylvania 15261, United States*; orcid.org/0000-0002-8679-9575; Email: lel55@pitt.edu

Complete contact information is available at: https://pubs.acs.org/10.1021/acs.langmuir.9b03865

Notes

The authors declare no competing financial interest.

Biographies

https://dx.doi.org/10.1021/acs.langmuir.9b03865
Langmuir 2020, 36, 2743–2756

Yali Wang received her B.S. in organic chemistry from China Agriculture University in 1997 and M.S. in inorganic chemistry from Peking University in 2001 (Beijing, China). She received her Ph.D. in physical chemistry from the University of Nebraska—Lincoln in 2015. She was a postdoctoral associate in structural biology at the University of Pittsburgh from 2015 to 2018. In 2018, she joined Yulin University as an associate professor. In 2019, she was a visiting scholar in Prof. Lei Li's group at the University of Pittsburgh. Her research interests are the interfacial behavior of ionic liquids on solid surfaces, wastewater reuse, and drug discovery.

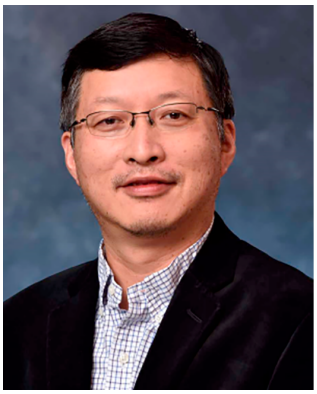

Lei Li received his B.S. and M.S. in polymer material from Tsinghua University (Beijing, China) in 1994 and 1997. He received his Ph.D. in macromolecular science and engineering from the University of Michigan in 2001. He joined Seagate Technology LLC in 2001. In 2010, he joined the Department of Chemical and Petroleum Engineering at the University of Pittsburgh, where he is now an associate professor. His research interests include surfaces, interfaces, and nanomaterials.

■ ACKNOWLEDGMENTS

Y.W. acknowledges the financial support of Yulin University startup funding (no. 18GK26) and the National Natural Science Foundation of China (no. 21763030). L.L. acknowledges the financial support from the National Science Foundation (CBET 1904486), the Advanced Storage Research Consortium (ASRC), and the University of Pittsburgh (CRDF). We thank Dr. Rui Qiao from Virginia Polytechnic Institute and State University for valuable discussions.

■ REFERENCES

(1) Dai, C.; Zhang, J.; Huang, C.; Lei, Z. Ionic liquids in selective oxidation: catalysts and solvents. *Chem. Rev.* **2017**, *117*, 6929−6983.
(2) Qiao, Y.; Ma, W.; Theyssen, N.; Chen, C.; Hou, Z. Temperature-responsive ionic liquids: fundamental behaviors and catalytic applications. *Chem. Rev.* **2017**, *117*, 6881−6928.
(3) Lei, Z. G.; Chen, B. H.; Koo, Y. M.; MacFarlane, D. R. Introduction: Ionic Liquids. *Chem. Rev.* **2017**, *117*, 6633−6635.
(4) Hayes, R.; Warr, G. G.; Atkin, R. Structure and Nanostructure in Ionic Liquids. *Chem. Rev.* **2015**, *115*, 6357−6426.
(5) Hayes, R.; Warr, G. G.; Atkin, R. At the interface: solvation and designing ionic liquids. *Phys. Chem. Chem. Phys.* **2010**, *12*, 1709−1723.
(6) Ray, A. Solvophobic interactions and micelle formation in structure forming nonaqueous solvents. *Nature* **1971**, *231*, 313.
(7) Parsegian, V. A.: *Van der Waals Forces: A Handbook for Biologists, Chemists, Engineers, and Physicists*; Cambridge University Press, 2005.
(8) Zhang, S.; Zhang, J.; Zhang, Y.; Deng, Y. Nanoconfined Ionic Liquids. *Chem. Rev.* **2017**, *117*, 6755−6833.
(9) Wan, M. M.; Zhu, H. Y.; Li, Y. Y.; Ma, J.; Liu, S.; Zhu, J. H. Novel CO2-capture derived from the basic ionic liquids orientated on mesoporous materials. *ACS Appl. Mater. Interfaces* **2014**, *6*, 12947−12955.
(10) Riisager, A.; Fehrmann, R.; Haumann, M.; Gorle, B. S.; Wasserscheid, P. Stability and kinetic studies of supported ionic liquid phase catalysts for hydroformylation of propene. *Ind. Eng. Chem. Res.* **2005**, *44*, 9853−9859.
(11) Hanna, D. G.; Shylesh, S.; Werner, S.; Bell, A. T. The kinetics of gas-phase propene hydroformylation over a supported ionic liquid-phase (SILP) rhodium catalyst. *J. Catal.* **2012**, *292*, 166−172.
(12) Shylesh, S.; Hanna, D.; Werner, S.; Bell, A. T. Factors influencing the activity, selectivity, and stability of Rh-based supported ionic liquid phase (SILP) catalysts for hydroformylation of propene. *ACS Catal.* **2012**, *2*, 487−493.
(13) Ueno, K.; Watanabe, M. From colloidal stability in ionic liquids to advanced soft materials using unique media. *Langmuir* **2011**, *27*, 9105−9115.
(14) Smith, J. A.; Werzer, O.; Webber, G. B.; Warr, G. G.; Atkin, R. Surprising particle stability and rapid sedimentation rates in an ionic liquid. *J. Phys. Chem. Lett.* **2010**, *1*, 64−68.
(15) Qiao, R. Water at ionic liquids-solid interfaces. *Current Opinion in Electrochemistry* **2019**, *13*, 11−17.
(16) Gebbie, M. A.; Smith, A. M.; Dobbs, H. A.; Warr, G. G.; Banquy, X.; Valtiner, M.; Rutland, M. W.; Israelachvili, J. N.; Perkin, S.; Atkin, R. Long range electrostatic forces in ionic liquids. *Chem. Commun.* **2017**, *53*, 1214−1224.
(17) Fedorov, M. V.; Kornyshev, A. A. Ionic liquids at electrified interfaces. *Chem. Rev.* **2014**, *114*, 2978−3036.
(18) Atkin, R.; Warr, G. G. Structure in confined room-temperature ionic liquids. *J. Phys. Chem. C* **2007**, *111*, 5162−5168.
(19) Bovio, S.; Podesta, A.; Lenardi, C.; Milani, P. Evidence of Extended Solidlike Layering in Bmim NTf2 Ionic Liquid Thin Films at Room-Temperature. *J. Phys. Chem. B* **2009**, *113*, 6600−6603.
(20) Perkin, S.; Albrecht, T.; Klein, J. Layering and shear properties of an ionic liquid, 1-ethyl-3-methylimidazolium ethylsulfate, confined to nano-films between mica surfaces. *Phys. Chem. Chem. Phys.* **2010**, *12*, 1243−1247.
(21) Yokota, Y.; Harada, T.; Fukui, K. I. Direct observation of layered structures at ionic liquid/solid interfaces by using frequency-modulation atomic force microscopy. *Chem. Commun.* **2010**, *46*, 8627−8629.
(22) Payal, R. S.; Balasubramanian, S. Effect of cation symmetry on the organization of ionic liquids near a charged mica surface. *J. Phys.: Condens. Matter* **2014**, *26*, 284101.
(23) Horn, R. G.; Israelachvili, J. N. Direct measurement of structural forces between two surfaces in a nonpolar liquid. *J. Chem. Phys.* **1981**, *75*, 1400−1411.
(24) Granick, S. Motions and relaxations of confined liquids. *Science* **1991**, *253*, 1374−1379.
(25) Israelachvili, J. N. *Intermolecular and Surface Forces*; Academic Press, 2015.
(26) Horn, R.; Evans, D.; Ninham, B. Double-layer and solvation forces measured in a molten salt and its mixtures with water. *J. Phys. Chem.* **1988**, *92*, 3531−3537.
(27) Carmichael, A. J.; Hardacre, C.; Holbrey, J. D.; Nieuwenhuyzen, M.; Seddon, K. R. Molecular layering and local order in thin films of 1-alkyl-3-methylimidazolium ionic liquids using X-ray reflectivity. *Mol. Phys.* **2001**, *99*, 795−800.
(28) Mezger, M.; Schröder, H.; Reichert, H.; Schramm, S.; Okasinski, J. S.; Schöder, S.; Honkimäki, V.; Deutsch, M.; Ocko, B. M.; Ralston, J. Molecular layering of fluorinated ionic liquids at a charged sapphire (0001) surface. *Science* **2008**, *322*, 424−428.
(29) Liu, Y.; Zhang, Y.; Wu, G.; Hu, J. Coexistence of liquid and solid phases of Bmim-PF6 ionic liquid on mica surfaces at room temperature. *J. Am. Chem. Soc.* **2006**, *128*, 7456−7457.
(30) Yokota, Y.; Harada, T.; Fukui, K.-i. Direct observation of layered structures at ionic liquid/solid interfaces by using frequency-modulation atomic force microscopy. *Chem. Commun.* **2010**, *46*, 8627−8629.

https://dx.doi.org/10.1021/acs.langmuir.9b03865
Langmuir 2020, 36, 2743−2756

(31) Ostendorf, F.; Schmitz, C.; Hirth, S.; Kühnle, A.; Kolodziej, J. J.; Reichling, M. How flat is an air-cleaved mica surface? *Nanotechnology* **2008**, *19*, 305705.
(32) Liu, Y. D.; Zhang, Y.; Wu, G. Z.; Hu, J. Coexistence of liquid and solid phases of Bmim-PF6 ionic liquid on mica surfaces at room temperature. *J. Am. Chem. Soc.* **2006**, *128*, 7456−7457.
(33) Hayes, R.; El Abedin, S. Z.; Atkin, R. Pronounced Structure in Confined Aprotic Room-Temperature Ionic Liquids. *J. Phys. Chem. B* **2009**, *113*, 7049−7052.
(34) Jurado, L. A.; Kim, H.; Arcifa, A.; Rossi, A.; Leal, C.; Spencer, N. D.; Espinosa-Marzal, R. M. Irreversible structural change of a dry ionic liquid under nanoconfinement. *Phys. Chem. Chem. Phys.* **2015**, *17*, 13613−13624.
(35) Perkin, S.; Crowhurst, L.; Niedermeyer, H.; Welton, T.; Smith, A. M.; Gosvami, N. N. Self-assembly in the electrical double layer of ionic liquids. *Chem. Commun.* **2011**, *47*, 6572−6574.
(36) Perkin, S. Ionic liquids in confined geometries. *Phys. Chem. Chem. Phys.* **2012**, *14*, 5052−5062.
(37) Bou-Malham, I.; Bureau, L. Nanoconfined ionic liquids: effect of surface charges on flow and molecular layering. *Soft Matter* **2010**, *6*, 4062−4065.
(38) Smith, A. M.; Lovelock, K. R. J.; Gosvami, N. N.; Licence, P.; Dolan, A.; Welton, T.; Perkin, S. Monolayer to Bilayer Structural Transition in Confined Pyrrolidinium-Based Ionic Liquids. *J. Phys. Chem. Lett.* **2013**, *4*, 378−382.
(39) Smith, A. M.; Lovelock, K. R. J.; Perkin, S. Monolayer and bilayer structures in ionic liquids and their mixtures confined to nano-films. *Faraday Discuss.* **2014**, *167*, 279−292.
(40) Griffin, L. R.; Browning, K. L.; Clarke, S. M.; Smith, A. M.; Perkin, S.; Skoda, M. W. A.; Norman, S. E. Direct measurements of ionic liquid layering at a single mica-liquid interface and in nano-films between two mica-liquid interfaces. *Phys. Chem. Chem. Phys.* **2017**, *19*, 297−304.
(41) Zhou, H.; Rouha, M.; Feng, G.; Lee, S. S.; Docherty, H.; Fenter, P.; Cummings, P. T.; Fulvio, P. F.; Dai, S.; McDonough, J. Nanoscale perturbations of room temperature ionic liquid structure at charged and uncharged interfaces. *ACS Nano* **2012**, *6*, 9818−9827.
(42) Jun, G. L. G.; Tabor, D. Surface adhesion and elastic properties of mica. *Nature* **1956**, *178*, 1304.
(43) Dragoni, D.; Manini, N.; Ballone, P. Interfacial Layering of a Room-Temperature Ionic Liquid Thin Film on Mica: A Computational Investigation. *ChemPhysChem* **2012**, *13*, 1772−1780.
(44) Perkin, S.; Salanne, M.; Madden, P.; Lynden-Bell, R. Is a Stern and diffuse layer model appropriate to ionic liquids at surfaces? *Proc. Natl. Acad. Sci. U. S. A.* **2013**, *110*, E4121−E4121.
(45) Zhou, H.; Rouha, M.; Feng, G.; Lee, S. S.; Docherty, H.; Fenter, P.; Cummings, P. T.; Fulvio, P. F.; Dai, S.; McDonough, J.; Presser, V.; Gogotsi, Y. Nanoscale Perturbations of Room Temperature Ionic Liquid Structure at Charged and Uncharged Interfaces. *ACS Nano* **2012**, *6*, 9818−9827.
(46) Smith, A. M.; Lovelock, K. R. J.; Gosvami, N. N.; Licence, P.; Dolan, A.; Welton, T.; Perkin, S. Monolayer to bilayer structural transition in confined pyrrolidinium-based ionic liquids. *J. Phys. Chem. Lett.* **2013**, *4*, 378−382.
(47) Gebbie, M. A.; Valtiner, M.; Banquy, X.; Fox, E. T.; Henderson, W. A.; Israelachvili, J. N. Ionic liquids behave as dilute electrolyte solutions. *Proc. Natl. Acad. Sci. U. S. A.* **2013**, *110*, 9674−9679.
(48) Hayes, R.; Warr, G. G.; Atkin, R. Structure and Nanostructure in Ionic Liquids. *Chem. Rev.* **2015**, *115*, 6357−6426.
(49) Triolo, A.; Russina, O.; Bleif, H.-J.; Di Cola, E. Nanoscale segregation in room temperature ionic liquids. *J. Phys. Chem. B* **2007**, *111*, 4641−4644.
(50) Gordon, C. M.; Holbrey, J. D.; Kennedy, A. R.; Seddon, K. R. Ionic liquid crystals: hexafluorophosphate salts. *J. Mater. Chem.* **1998**, *8*, 2627−2636.
(51) Paradies, H. H.; Habben, F. Structure of N-hexadecylpyridinium chloride monohydrate. *Acta Crystallogr., Sect. C: Cryst. Struct. Commun.* **1993**, *49*, 744−747.
(52) Henderson, W. A.; Fylstra, P.; Hugh, C.; Trulove, P. C.; Parsons, S. Crystal structure of the ionic liquid EtNH 3 NO 3—Insights into the thermal phase behavior of protic ionic liquids. *Phys. Chem. Chem. Phys.* **2012**, *14*, 16041−16046.
(53) Wang, Y.; Voth, G. A. Unique spatial heterogeneity in ionic liquids. *J. Am. Chem. Soc.* **2005**, *127*, 12192−12193.
(54) Urahata, S. M.; Ribeiro, M. C. C. Structure of ionic liquids of 1-alkyl-3-methylimidazolium cations: A systematic computer simulation study. *J. Chem. Phys.* **2004**, *120*, 1855−1863.
(55) Deyko, A.; Cremer, T.; Rietzler, F.; Perkin, S.; Crowhurst, L.; Welton, T.; Steinruck, H. P.; Maier, F. Interfacial Behavior of Thin Ionic Liquid Films on Mica. *J. Phys. Chem. C* **2013**, *117*, 5101−5111.
(56) Wakeham, D.; Hayes, R.; Warr, G. G.; Atkin, R. Influence of temperature and molecular structure on ionic liquid solvation layers. *J. Phys. Chem. B* **2009**, *113*, 5961−5966.
(57) Elbourne, A.; Voitchovsky, K.; Warr, G. G.; Atkin, R. Ion structure controls ionic liquid near-surface and interfacial nanostructure. *Chemical Science* **2015**, *6*, 527−536.
(58) Segura, J. J.; Elbourne, A.; Wanless, E. J.; Warr, G. G.; Voïtchovsky, K.; Atkin, R. Adsorbed and near surface structure of ionic liquids at a solid interface. *Phys. Chem. Chem. Phys.* **2013**, *15*, 3320−3328.
(59) Cheng, H. W.; Stock, P.; Moeremans, B.; Baimpos, T.; Banquy, X.; Renner, F. U.; Valtiner, M. Characterizing the Influence of Water on Charging and Layering at Electrified Ionic-Liquid/Solid Interfaces. *Adv. Mater. Interfaces* **2015**, *2*, 1500159.
(60) Gong, X.; Kozbial, A.; Li, L. What causes extended layering of ionic liquids on the mica surface? *Chemical Science* **2015**, *6*, 3478−3482.
(61) Gong, X.; Li, L. Understanding the wettability of nanometer-thick room temperature ionic liquids (RTILs) on solid surfaces. *Chin. Chem. Lett.* **2017**, *28*, 2045−2052.
(62) Gong, X.; Wang, B. C.; Kozbial, A.; Li, L. From Molecular Arrangement to Macroscopic Wetting of Ionic Liquids on the Mica Surface: Effect of Humidity. *Langmuir* **2018**, *34*, 12167−12173.
(63) Singh, T.; Kumar, A. Static dielectric constant of room temperature ionic liquids: internal pressure and cohesive energy density approach. *J. Phys. Chem. B* **2008**, *112*, 12968−12972.
(64) Jiang, W.; Wang, Y.; Voth, G. A. Molecular dynamics simulation of nanostructural organization in ionic liquid/water mixtures. *J. Phys. Chem. B* **2007**, *111*, 4812−4818.
(65) Firestone, M. A.; Dzielawa, J. A.; Zapol, P.; Curtiss, L. A.; Seifert, S.; Dietz, M. L. Lyotropic liquid-crystalline gel formation in a room-temperature ionic liquid. *Langmuir* **2002**, *18*, 7258−7260.
(66) Cheng, H. W.; Dienemann, J. N.; Stock, P.; Merola, C.; Chen, Y. J.; Valtiner, M. The Effect of Water and Confinement on Self-Assembly of Imidazolium Based Ionic Liquids at Mica Interfaces. *Sci. Rep.* **2016**, *6*, 30058.
(67) Wang, Z.; Shi, F.; Zhao, C. Humidity-accelerated spreading of ionic liquids on a mica surface. *RSC Adv.* **2017**, *7*, 42718−42724.
(68) Lhermerout, R.; Perkin, S. A new methodology for a detailed investigation of quantized friction in ionic liquids. *Phys. Chem. Chem. Phys.* **2020**, *22*, 455.
(69) McDonald, S.; Elbourne, A.; Warr, G. G.; Atkin, R. Metal ion adsorption at the ionic liquid−mica interface. *Nanoscale* **2016**, *8*, 906−914.
(70) Varela, L.; Carrete, J.; García, M.; Gallego, L.; Turmine, M.; Rilo, E.; Cabeza, O. Pseudolattice theory of charge transport in ionic solutions: Corresponding states law for the electric conductivity. *Fluid Phase Equilib.* **2010**, *298*, 280−286.
(71) Kawada, S.; Kodama, E.; Sato, K.; Ogawa, S.; Watanabe, M.; Okubo, H.; Sasaki, S. Effect of water on the interfacial structures of room-temperature ionic liquids. *Surf. Interface Anal.* **2019**, *51*, 17−20.
(72) Samanta, A. Solvation dynamics in ionic liquids: what we have learned from the dynamic fluorescence stokes shift studies. *J. Phys. Chem. Lett.* **2010**, *1*, 1557−1562.
(73) Baker, S. N.; Baker, G. A.; Munson, C. A.; Chen, F.; Bukowski, E. J.; Cartwright, A. N.; Bright, F. V. Effects of solubilized water on the relaxation dynamics surrounding 6-propionyl-2-(N, N-dimethylamino)

naphthalene dissolved in 1-butyl-3-methylimidazolium hexafluorophosphate at 298 K. *Ind. Eng. Chem. Res.* **2003**, *42*, 6457−6463.
(74) Chakrabarty, D.; Chakraborty, A.; Seth, D.; Sarkar, N. Effect of water, methanol, and acetonitrile on solvent relaxation and rotational relaxation of coumarin 153 in neat 1-hexyl-3-methylimidazolium hexafluorophosphate. *J. Phys. Chem. A* **2005**, *109*, 1764−1769.
(75) Sakai, K.; Okada, K.; Uka, A.; Misono, T.; Endo, T.; Sasaki, S.; Abe, M.; Sakai, H. Effects of Water on Solvation Layers of Imidazolium-Type Room Temperature Ionic Liquids on Silica and Mica. *Langmuir* **2015**, *31*, 6085−6091.
(76) Wang, Z.; Li, H.; Atkin, R.; Priest, C. Influence of water on the interfacial nanostructure and wetting of [Rmim][NTf2] ionic liquids at mica surfaces. *Langmuir* **2016**, *32*, 8818−8825.
(77) Jurado, L. A.; Kim, H.; Rossi, A.; Arcifa, A.; Schuh, J. K.; Spencer, N. D.; Leal, C.; Ewoldt, R. H.; Espinosa-Marzal, R. M. Effect of the environmental humidity on the bulk, interfacial and nanoconfined properties of an ionic liquid. *Phys. Chem. Chem. Phys.* **2016**, *18*, 22719−22730.
(78) Sakai, K.; Okada, K.; Misono, T.; Endo, T.; Abe, M.; Sakai, H. Characterizing solid/ionic liquid interfaces in the presence of water and nonionic surfactants. *Colloids Surf., A* **2016**, *509*, 433−439.
(79) Smith, A. M.; Perkin, S. Switching the structural force in ionic liquid-solvent mixtures by varying composition. *Phys. Rev. Lett.* **2017**, *118*, 096002.
(80) Yang, X.; Cheng, C.; Wang, Y.; Qiu, L.; Li, D. Liquid-mediated dense integration of graphene materials for compact capacitive energy storage. *Science* **2013**, *341*, 534−537.
(81) Raviv, U.; Laurat, P.; Klein, J. Fluidity of water confined to subnanometre films. *Nature* **2001**, *413*, 51.
(82) Raviv, U.; Perkin, S.; Laurat, P.; Klein, J. Fluidity of water confined down to subnanometer films. *Langmuir* **2004**, *20*, 5322−5332.
(83) Gong, X.; Wang, B.; Li, L. Spreading of Nanodroplets of Ionic Liquids on the Mica Surface. *ACS Omega* **2018**, *3*, 16398−16402.
(84) Wang, Z.; Priest, C. Impact of nanoscale surface heterogeneity on precursor film growth and macroscopic spreading of [Rmim][NTf2] ionic liquids on mica. *Langmuir* **2013**, *29*, 11344−11353.

https://dx.doi.org/10.1021/acs.langmuir.9b03865
Langmuir 2020, 36, 2743−2756